MOL PHARM

MOLECULAR PHARMACOLOGY

Antitumor Activity of the Retinoid-Related Molecules (E)-3-(4′-Hydroxy-3′-adamantylbiphenyl-4-yl)acrylic Acid (ST1926) and 6-[3-(1-Adamantyl)-4-hydroxyphenyl]-2-naphthalene Carboxylic Acid (CD437) in F9 Teratocarcinoma: Role of Retinoic Acid Receptor γ and Retinoid-Independent Pathways[S]

Edoardo Parrella, Maurizio Giannì, Maddalena Fratelli, Maria Monica Barzago, Ivan Raska Jr, Luisa Diomede, Mami Kurosaki, Claudio Pisano, Paolo Carminati, Lucio Merlini, Sabrina Dallavalle, Michele Tavecchio, Cecile Rochette-Egly, Mineko Terao, and Enrico Garattini

Laboratory of Molecular Biology, Centro Catullo e Daniela Borgomainerio (M.G., M.F., M.M.B., I.R., L.D., M.K., M.Te., E.G.) and Department of Oncology (M.Ta.), Istituto di Ricerche Farmacologiche "Mario Negri", Milano, Italy; Sigma-Tau Industrie Farmaceutiche Riunite, Pomezia, Italy (C.P., P.C.); Dipartimento di Scienze Molecolari Agroalimentari, Università degli Studi di Milano, Milano, Italy (L.M., S.D.); and Institut de Genetique et Biologie Moleculaire, Illkirch, France (C.R.-E., E.P.)

ABSTRACT

The retinoid-related molecules (RRMs) ST1926 [(E)-3-(4′-hydroxy-3′-adamantylbiphenyl-4-yl)acrylic acid] and CD437 (6-[3-(1-adamantyl)-4-hydroxyphenyl]-2-naphthalene carboxylic acid) are promising anticancer agents. We compared the retinoic acid receptor (RAR) trans-activating properties of the two RRMs and all-trans-retinoic acid (ATRA). ST1926 and CD437 are better RARγ agonists than ATRA. We used three teratocarcinoma cell lines to evaluate the significance of RARγ in the activity of RRMs: F9-wild type (WT); F9γ−/−, lacking the RARγ gene; F9γ51, a F9γ−/− derivative, complemented for the RARγ deficit. Similar to ATRA, ST1926 and CD437 activate cytodifferentiation only in F9-WT cells. Unlike ATRA, ST1926 and CD437 arrest cells in the G₂/M phase of the cell cycle and induce apoptosis in all F9 cell lines. Our data indicate that RARγ and the classic retinoid pathway are not relevant for the antiproliferative and apoptotic activities of RRMs in vitro. Increases in cytosolic calcium are fundamental for apoptosis, in that intracellular calcium chelators abrogate the process. Comparison of the gene expression profiles associated with ST1926 and ATRA in F9-WT and F9γ−/− indicates that the RRM activates a conspicuous nonretinoid response in addition to the classic and RAR-dependent pathway. The pattern of genes regulated by ST1926 selectively, in a RARγ-independent manner, provides novel insights into the possible molecular determinants underlying the activity of RRMs in vitro. Furthermore, it suggests that RARγ-dependent responses are relevant to the activity of RRMs in vivo. Indeed, the receptor hinders the antitumor activity in vivo, in that both syngeneic and immunosuppressed SCID mice bearing F9γ−/− tumors have increased life spans after treatment with ST1926 and CD437 relative to their F9-WT counterparts.

All-trans-retinoic acid (ATRA) and derivatives (retinoids) are promising antineoplastic agents (Garattini and Terao, 2004; Garattini et al., 2004b). The activity of classic retinoids is the consequence of selective antiproliferative and cytodifferentiating effects that are mediated predominantly by specific nuclear receptors of the RAR and RXR families (Altucci and Gronemeyer, 2001). In many cell types, classic retinoids

ABBREVIATIONS: ATRA, all-trans-retinoic acid; RAR, retinoic acid receptor; RXR, retinoid X receptor; RRM, retinoid-related molecule; CD437, (E)-3-(4′-hydroxy-3′-adamantylbiphenyl-4-yl)acrylic acid; ST1926, 6-[3-(1-adamantyl)-4-hydroxyphenyl]-2-naphthalene carboxylic acid; BAPTA, 1,2 bis (2-aminophenoxy)ethane-N,N,N′,N′-tetraacetic acid tetrakis (acetoxymethyl ester); FURA-2, Fura-2 acetoxymethyl ester; DEVD-amc, N-acetyl-Asp-Glu-Val-Asp-amino-4-methylcoumarin; PBS, phosphate-buffered saline; PI, propidium iodide; RT-PCR, reverse transcription-polymerase chain reaction; DMSO, dimethyl sulfoxide; ANOVA, analysis of variance; WT, wild-type; FACS, fluorescence-activated cell sorting; TNF, tumor necrosis factor; AV, annexin V.

exert unique actions of oncological interest, including growth inhibition, cytodifferentiation, and direct or indirect cytotoxicity. Because the molecular mechanisms of action of retinoids are generally different from those of other antineoplastic agents, there is growing interest in the synthesis of molecules with new properties (Rishi et al., 2003; Sabichi et al., 2003; Cao et al., 2004; Chun et al., 2005).

A novel series of synthetic retinoic acid derivatives [retinoid-related molecules (RRMs) or atypical retinoids], with activity in leukemia and cancer cells, has been described recently (Mologni et al., 1999; Ponzanelli et al., 2000; Sun et al., 2002; Zhang et al., 2002; Garattini et al., 2004a; Lopez-Hernandez et al., 2004; Zuco et al., 2004). In certain cellular contexts, these molecules do not show cross-resistance with ATRA (Marchetti et al., 1999) and other chemotherapeutics (Ponzanelli et al., 2000), suggesting novel features and mechanisms of action relative to classic retinoids and the available anticancer agents. The prototypes of RRMs are CD437 and ST1926 (Garattini et al., 2004). CD437 is a retinoid originally developed as a selective RARγ agonist (Delescluse et al., 1991). Although a preliminary report suggested that ST1926 is not an efficient RARγ agonist (Cincinelli et al., 2003), we have provided evidence that the compound does bind to and trans-activate the receptor (Garattini et al., 2004b). ST1926 is a more powerful antileukemic and anticancer agent (Cincinelli et al., 2003; Garattini et al., 2004a) with better toxicologic and pharmacokinetic profiles than CD437. ST1926 is under preclinical development in view of phase I clinical trials.

Various aspects of the molecular mechanisms of action of RRMs remain unclear. From a structural standpoint, RRMs are classified as synthetic retinoids. However, the contribution of nuclear retinoic acid receptors to the antineoplastic activity of ST1926 and CD437 is not completely defined. In particular, involvement of RARγ is debated (Hsu et al., 1997; Holmes et al., 2000; Sun et al., 2000a; Zhao et al., 2001). In certain cells, pharmacological inhibition of RARγ blocks the action of CD437 (Holmes et al., 2000), whereas in others, this is ineffective (Mologni et al., 1999). Synthesis of an active RRM with strong apoptotic properties and no RARγ binding activity (Dawson et al., 2001) adds to the controversy. Furthermore, although the activity of ST1926 and CD437 in myeloid leukemia is predominantly the result of an apoptotic process, RRMs also inhibit growth and induce cytodifferentiation in other tumor contexts. These two further actions may contribute to the overall antineoplastic activity of RRMs and have never been the object of a systematic study. Finally, the gene expression program set in motion by RRMs and its dependence on the activation of RARγ or other RAR isotypes is unknown.

F9 teratocarcinoma cells represent a useful cell-autonomous model to study the activity of retinoids (Boylan et al., 1993; Taneja et al., 1997; Faria et al., 1999; Rochette-Egly et al., 2000a,b; Rochette-Egly and Chambon, 2001; Zhuang et al., 2003; Bour et al., 2005). These cells undergo growth arrest and differentiation along the primitive endoderm in response to ATRA and other synthetic retinoids. Moreover, studies conducted with F9 sublines presenting genetic deletion of RARγ (Boylan et al., 1993) demonstrated that endodermal differentiation requires activation of the receptor. Thus, the F9 model is well suited to define the relative contribution of cytodifferentiation and growth inhibition to

the overall antineoplastic activity of RRMs. Furthermore, the use of F9 teratocarcinoma cells is likely to provide information as to the relevance of the classic RAR/RXR and alternative or complementary pathways for the pharmacology of RRMs. Finally, the availability of F9 teratocarcinoma cell lines differing only in the expression of RARγ (Taneja et al., 1997) represents a unique tool to study the significance of the receptor for the antineoplastic activity of RRMs. The growth of F9 teratocarcinoma cells as solid tumors in syngenic strains of animals is a further advantage, permitting in vivo experiments.

In this study, three F9 teratocarcinoma cell lines with different expression of RARγ were used to investigate the cytodifferentiating, antiproliferative, and apoptotic effects of ST1926 and CD437 compared with ATRA. In the same system, using whole-genome microarrays, ST1926 specific responses and their RARγ-dependence were defined. Finally, the involvement of RARγ in the overall antitumor activity of RRMs was studied in normal and immunosuppressed mice transplanted with F9 cells.

Materials and Methods

Chemicals. ATRA and BAPTA were purchased from Sigma (St. Louis, MO). Fura-2 acetoxymethyl ester (FURA-2) was from Invitrogen (Carlsbad, CA). ST1926 and CD437 were synthesized by Sigma-Tau Industrie Farmaceutiche Riunite S.p.a. (Pomezia, Italy).

Cell Cultures and Transfections. COS-7 (American Type Culture Collection, Manassas, VA) and the F9 teratocarcinoma cell lines, F9-WT, F9γ−/−, and F9γ51 (Taneja et al., 1997), were grown in Dulbecco's modified Eagle's medium containing 10% fetal calf serum and were free from mycoplasma. COS-7 cells were transfected with human RARα, RARβ, RARγ, or RXRα pSG5-based plasmids along with the DR5-tk-CAT (RAR-dependent) or DR1-tk-CAT (RXR-dependent) reporter genes and the normalization plasmid pCH110 (β-galactosidase) (Garattini et al., 2004a). Transactivation assays on the various isoforms of RAR were performed using extracts of transfected COS-7 treated for 24 h with different concentrations of the test retinoid, as described previously (Garattini et al., 2004a)

Cellular Proliferation, Viability, and Apoptosis. Cell number and viability were determined after staining with erythrosin (Sigma). For the determination of the apoptotic index, adherent cells were detached, fixed in methanol, and stained with 4,6 diamidino-2-phenylindole (Giannì et al., 2000). The apoptotic index is the percentage of cells with features of nuclear fragmentation after counting a minimum of 300 nuclei/field under the fluorescence microscope. In some experiments, apoptosis was determined according to the Annexin-V assay by flow cytometry (Mebcyto Apoptosis Kit; MBL International, Woburn, MA) (Garattinì et al., 2004a), using the flow cytometer FACSCalibur (BD Biosciences, Palo Alto, CA). Caspase-3 activation was measured with the fluorogenic peptide substrate DEVD-amc (N-acetyl-Asp-Glu-Val-Asp-amino-4-methylcoumarin; Alexis, Laufelingen, Switzerland) (Mologni et al., 1999).

Flow Cytometric Cell Cycle Analysis. F9-WT and F9γ−/− cells were counted using a Coulter counter (Beckman Coulter, Fullerton, CA) and fixed in 70% ethanol. Cells ($1–2 \times 10^6$) were washed with PBS and stained with 1 ml of a solution containing 10 μg/ml propidium iodide (PI) and 10,000 units of RNase overnight at 4°C in the dark. Flow cytometric analyses were performed using FACSCalibur, and the distribution of the cells in the different cell cycle phases calculated by the gaussian method (Ubezio, 1985).

RNA Preparation and RT-PCR. Total RNA was extracted according to the guanidinium-thiocyanate-cesium chloride method, reverse transcribed, and amplified by polymerase chain reaction (PCR) using synthetic amplimers (GeneAmp RNA-PCR core kit; Applied

Biosystems Inc., Branchburg, NJ). The amplimers used are shown in Table 1.

Real-time RT-PCR was performed using Taqman gene expression assays (Applied Biosystems, Foster City, CA) following the manufacturer's instructions, on a GeneAmp 5700 sequence detector (Applied Biosystems). The assays used were Mm00439359_m1, with primers located at the 1-2 exon boundary of the *HOXA1* gene; Mm00487803_m1, with primers located at the 1-2 exon boundary of the c-*myc* gene; Mm00445212_m1, located at the 7-8 exon boundary of the KIT oncogene; Mm01319677_m1, located at the 4-5 exon boundary of the *RARβ* gene; and Mm00435270, located at the 19-20 exon boundary of the Notch homolog 3 gene. The β-actin housekeeping gene (assay ID Mm00607939_s1) was used for the normalization of the results.

Measurement of Intracellular Calcium. Changes in intracellular calcium concentrations were measured at the single-cell level in a semiquantitative fashion. In brief, F9-WT or F9γ−/− cells were seeded (300,000/ml) on microscopic glass slides and allowed to adhere overnight. Cells were labeled with 4 μM Fluo3-AM (Invitrogen) at 37°C for 1 h. Slides were washed twice with PBS and incubated in PBS containing 1.26 mM CaCl2. After addition of vehicle (DMSO) or ST1926 (1 μM) the associated fluorescence was measured for a maximum of 1 h with an IX70 microscope (Olympus, Hamburg, Germany) equipped with an imaging system (Till Photonics GMBH, Gräfelfing, Germany). For each experiment, cells were scanned for at least 30 s to establish a baseline fluorescence reading before addition of the appropriate stimulus. All incubations were carried out while continuously scanning the cells every 200 ms.

For the quantitative determination of intracellular calcium in the entire cell population, a previously described protocol was used (Garattini et al., 2004a). For these experiments, the FURA-2-associated fluorescence was measured continuously at $37 \pm 1°C$ with a spectro-photofluorometer (LS-50B; PerkinElmer Life and Analytical Sciences, Milano, Italy).

In Vivo Studies. F9-WT or F9γ−/− cells (3×10^6) were inoculated intraperitoneally in 129/Sv syngenic animals or in immunodeficient SCID mice (Charles River Italia, Calco, Italy). ST1926, CD437, or ATRA was dissolved in a diluent consisting of cremophor/ethanol (Garattini et al., 2004a). All the compounds were administered i.p. or orally once per day for up to 3 weeks. Body weight and lethality were recorded every day. All the experiments were approved by the Internal Animal Care Committee and conducted according to the pertinent International and Italian legislation.

Gene Microarrays. F9-WT and F9γ−/− were treated for 10 h with vehicle (DMSO), all-*trans*-retinoic acid (0.5 μM), or the synthetic retinoid ST1926 (0.5 μM). The polyadenylated RNA fraction was isolated from total RNA using magnetic oligo(dT) micro-spheres (DYNAL AS, Oslo, Norway). Polyadenylated RNA was amplified and labeled with the fluorochrome Cy3 or Cy5 using the Amino allyl MessageAMP II kit (Ambion Inc., Austin, TX). Each RNA preparation represents a pool of four flasks treated independently with the appropriate stimulus. Each experimental sample consists of 1) a replicate in which the control RNA is labeled with Cy3 and the treated RNA with Cy5 and 2) a swapped replicate in which the control RNA is labeled with Cy3 and the treated RNA with Cy5. An equal amount of Cy3- and Cy5-labeled cRNAs were mixed and hybridized to the oligonucleotide microarray (Agilent 60-mer microarray oligo processing protocol version 2.1; Agilent Technologies, Palo Alto, CA). After washing, microarray glass slides were scanned with the G2565AA dual laser scanner (Agilent Technologies). Images were analyzed with the Feature Extraction software version 7.1 (Agilent Technologies). Dye normalization was performed automatically, using the Rank Consistency filter and the LinearLOWESS normalization method. The raw data of the microarray experiments

TABLE 1
Amplimers

	Sequence	Nucleotides	GenBank Accession No.
Collagen type IV	5′-ATCAACAACGTCTGCAACTTCGCC-3′	4649–4672	J04694
Complementary	5′-TTCTTCTCATGCACACTTGGCAGC-3′	5113–5136	
Laminin B1 subunit 1	5′-AGAGCTGAGCTGTTGCTTGAGGAA-3′	4885–4908	NM_008482
Complementary	5′-TGCTGTTAGCTTGAGCCAAGAGTG-3′		
Notch Hom.3	5′-CTCAGCTTTGGTCTGCTCAATCCT-3′	6531–6554	NM_008716
Complementary	5′-CTGAGGGAGGGAGGGAACAGATAT-3′	7033–7056	
Apaf1	5′-GTGTGGAATGTCATTACCGGAA-3′	3756–3777	NM_009684
Complementary	5′-CGAGATTATCGACAGTCACATAGGTT-3′	4245–4270	
Ddit4	5′-CTGCTAAGTGATTTCGACTACTGGG-3′	283–307	NM_030143
Complementary	5′-GTCGTTCCAATCAGGGAGTACAG-3′	742–764	
Na Channel IIIβ	5′-AGATGCATCTCCTGCATGAAGAG-3′	361–383	NM_178227
Complementary	5′-ACCACAGAGTTCTCCTTGTTCTCTG-3′	839–863	
Caveolin 2	5′-AGAAGGCCGATGTGCAGCTCTTCA-3′	37–60	NM_016900
Complementary	5′-CAGTTGCATGCTGACCGATGAGAA-3′	474–497	
Kit oncogene	5′-ATCATGGAAGATGACGAGCTGGCT-3′	2288–2311	NM_021099
Complementary	5′-GCTGTCCGAGATCTGCTTCTCAAT-3′	2792–2815	
CYP26a1	5′-CTGCGACATCACTGATCACTTACC-3′	979–1002	NM_007811)
Complementary	5′-CTGGAAGTAGGTGAATCTTGCAGG-3′	1515–1538	
c-myc	5′-CAGCGCACTCTGAAGAAGAGCAAGA-3′	1353–1376	NM_010849
Complementary	5′-TGAGCTTGTGCTCGTCTGCTTGAA-3′	1823–1846	
Homeobox B2	5′-CGAAAGGCAGGTCAAAGTCTGGTT-3′	307–330	NM_134032
Complementary	5′-GAAACTGCAAGTCGATGGCACAGA-3′	801–824	
RARα	5′-GAACATGGTGTATACGTGTCACCG-3′	758–781	NM_009024
Complementary	5′-TCAATGTCCAGGGAGACTCGTTGT-3′	1049–1072,	
RARβ	5′-AGAGAGCTATGAGATGACAGCGGA-3′	700–723	NM_011243
Complementary	5′-GAAAGTCATGGTGTCTTGCTCTGG-3′	1010–1033	
RARγ	5′-TGGAGACACAGAGCACCAGCTC-3′	440–461	NM_011244
Complementary	5′-TCCGAGAATGTCATAGTGTCCTGC-3′	1098–1121	
RXRα	5′-AAGGACTGCCTGATCGACAAGAGA-3′	705–738	NM_011305
Complementary	5′-TGAAGAGCTGCTTGTCTGCTGCTT-3′	1001–1024	
RXRβ	5′-ACCTGACCTACTCGTGTCGTGATA-3′	814–837	NM_011306
Complementary	5′-TTGTCTAGCTGCCTGGCAGATGTTA-3′	1118–1141	
RXRγ	5′-AGATTGTCTCATCGACAAGCGCCA-3′	909–932	NM_009107
Complementary	5′-CCTCCAAGGTGAGATCTGAGAAGT-3′	1238–1261	

were deposited in the public database Miamexpress (http://www.ebi.ac.uk/miamexpress) with the accession number E-MEXP-361. Further Qspline normalization (Workman et al., 2002) of the intensity data was conducted using Gene Publisher (Knudsen et al., 2003). Two-way ANOVA based on F distribution (factor A: vehicle, ST1926, or ATRA; factor B: F9-WT or F9γ−/−) was performed with the T-MEV software (Saeed et al., 2003; http://www.tm4.org/mev.html). Significant genes ($p < 0.0001$) were classified based on Pavlidis template-matching algorithm and hierarchical clustering using Pearson correlation as the distance measure (Pavlidis and Noble, 2001; Kasturi et al., 2003).

Results

ST1926 and CD437 Were RARγ Activators. We compared the ability of ST1926, CD437, and ATRA to activate RARα, RARβ, and RARγ overexpressed in COS-7 cells (Table 2). The EC_{50} reflects the affinity of each retinoid for the three isoforms of RAR. For RARα and RARβ, the rank order of potency was ATRA = CD437 > ST1926, whereas for RARγ, it was CD437 > ATRA > ST1926. RAR selectivity was calculated as the inverse ratio of the EC_{50} values. The data obtained are consistent with previous results, indicating that ATRA was a nonselective (pan-RAR) agonist, whereas CD437 was a selective RARγ agonist. In addition, our results demonstrated that ST1926 bound and trans-activated the three receptors with similar affinity and, unlike CD437, lacked RARγ selectivity. Table 2 also shows the maximal activity of each compound at saturating concentrations. It is noteworthy that both ST1926 and CD437 activated RARγ more efficiently than ATRA. Cotransfection of RXRα did not change the EC_{50} values of ST1926, CD437, and ATRA for the various isoforms of RAR (data not shown). This is in line with the concept that COS-7 cells contain significant amounts of native RXRs that combine with overexpressed RARs to form transcriptionally active RXR/RAR heterodimers (Garattini et al., 2004b; Giannì et al., 2006).

ST1926 and CD437 are unlikely to possess significant RXR agonistic activity, as demonstrated by transfection of COS-7 cells with RXRα and an appropriate reporter gene activated by RXR/RXR homodimers. Under these experimental conditions, the RXR agonist 9-*cis* retinoic acid (1 μM) caused a

9.7 ± 0.8 (mean ± S.D., $n = 3$) induction of CAT reporter activity over the unliganded control sample. In contrast, the effects of ST1926 or CD437 were minimal, dose-independent, and did not exceed a 2-fold induction at all the concentrations investigated (0.01 μM-10 μM).
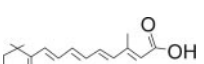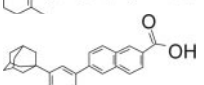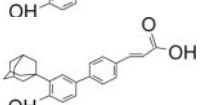
The F9 Teratocarcinoma Model. To define the relevance of nuclear retinoic acid receptors, and RARγ in particular, for the pharmacological activity of ST1926 and CD437, we chose the mouse F9 teratocarcinoma model. Experiments were performed on three clonal cell lines with different expression of RARγ. As shown in Fig. 1A, wild-type F9 cells (F9-WT) expressed RARα and RARγ constitutively. As expected, RARβ was not expressed under basal conditions. Ablation of the RARγ gene by homologous recombination results in an F9 subline (F9γ−/−), which maintains synthesis of RARα but has an absolute deficit of RARγ (Boylan et al., 1993). RARγ expression in the F9γ−/− cellular background is partially reconstituted by transgenesis in F9γ51 cells (Taneja et al., 1997).

Figure 1B demonstrates that the proliferation curves of F9-WT and F9γ−/− cell lines in standard culture conditions were very similar. Furthermore, the growth of the two cell types did not differ significantly from that determined for RARγ51. Finally, the morphology of the three lines growing in basal conditions is indistinguishable (data not shown). The similarities of F9-WT and F9γ−/− cells in vitro are recapitulated in vivo. Figure 1C illustrates the growth characteristics and the morphology of the tumors derived from the F9-WT and F9γ−/− cells in syngeneic 129/Sv mice. The two types of tumors grew as homogeneous solid masses in the peritoneal cavity and had similar and highly undifferentiated cell morphology. The growth kinetics of the two tumors were superimposable and resulted in masses of similar weight and volume. The median survival times of animals inoculated with F9-WT and F9γ−/− cells did not differ significantly and were 14.3 ± 3.2 and 13.0 ± 3.1 days (mean ± SD of three independent experiments), respectively. All together, our results indicate that RARγ expression had no influence on the in vitro or in vivo growth and morphology of

TABLE 2
Nuclear retinoic acid receptor specificity of RRMs

COS-7 cells (200,000/well) were transfected with expression vectors containing the indicated RAR isoforms (0.1 μg), a DR5-tk-reporter construct (1.0 μg) and pCH110 normalizing vector containing bacterial β-galactosidase (0.5 μg). Twenty-four hours after transfection, cells were treated for further 24 h with different concentrations of the retinoid (0.0001–10 μM), using logarithmic dilutions. CAT activity was measured in cell extracts and normalized for the level of transfection using β-galactosidase enzymatic activity. The Ec50 (the concentration giving 50% of the maximal transactivation effect) was obtained from appropriate dose-response curves run in duplicate and was calculated with the Prism version 4.0 software package (GraphPad Software, San Diego, CA). Receptor selectivity is calculated as the inverse ratio of the Ec50s determined for each couple of receptors. Each value is the mean + SD of 3 independent transfection replicates. The maximal activity is relative to ATRA, whose transactivation effect is taken as 100. This parameter is expressed as the % ratio of the CAT activity measured for each compound (1 mM) and ATRA (1 mM) after transfection of the indicated isoform. Each value is the mean + SD of 3 independent transfection replicates.

Compound		EC_{50}			Receptor Selectivity			Maximal Activity (1 μM)		
		RARα	RARβ	RARγ	RARγ/α	RARγ/β	RARα/β	RARα	RARβ	RARγ
			μM							
ATRA		0.02 (0.01–0.04)	0.05 (0.04–0.07)	0.03 (0.02–0.05)	0.9	1.7	2.1	100	100	100
CD437		0.06 (0.05–0.55)	0.05 (0.04–0.08)	0.003 (0.002–0.004)	21.5	16.0	0.8	175 ± 8	176 ± 10	453 ± 30
ST1926		0.16 (0.13–0.25)	0.14 (0.04–0.25)	0.14 (0.12–0.17)	1.2	1.0	0.9	201 ± 20	231 ± 9	412 ± 30

untreated F9 cells. These features support the relevance of the model for our comparative studies on RRMs and ATRA.

ST1926 and CD437, Like ATRA, Induce F9 Cytodifferentiation via RARγ. To study cytodifferentiation, we compared the ability of ATRA, ST1926, and CD437 to induce the expression of the mRNAs coding for two validated markers of the primitive endoderm, collagen IV and laminin B in F9-WT and F9γ−/− (Fig. 2A). As expected, the synthesis of the collagen IV and laminin B transcripts was induced in F9-WT cells treated with ATRA (0.1 μM) for 48 h but not in

Fig. 1. RAR expression, proliferation, and differentiation of F9-WT, F9γ−/−, and F9γ51 cell lines. A, cell extracts were prepared from logarithmically growing F9-WT, F9γ−/−, and F9γ51 cells. Extracts of COS-7 cells transfected with RARα and RARβ cDNAs were used as positive controls. Western blot analyses were conducted with specific anti-RARα, RARβ, RARγ, and β-actin polyclonal antibodies. B, the proliferation curves of the indicated cell lines grown in complete medium are shown. The results are the mean ± S.D. of three replicate cell cultures. C, the bar graph shows the weight of the F9-WT and F9γ−/− tumors 10 days after i.p. transplantation of the corresponding cells (3×10^6/animal). The results are the mean ± S.D. of the tumor masses determined in 10 animals. The photographs illustrate the microscopic morphology of the F9-WT and F9γ−/− tumors after hematoxylin-eosin staining of representative tissue slices.

the F9γ−/− counterpart. Both ST1926 and CD437 (0.1 μM) were at least as effective as ATRA in inducing the two marker mRNAs; once again, this phenomenon was evident only in the F9-WT cell line. Hence, under the experimental conditions considered, the two RRMs acted as classic retinoids and induced primitive endodermal differentiation in a RARγ-dependent mode. Our results are consistent with the fact that RARγ expression is necessary for the retinoid-dependent differentiation of F9 into primitive endodermal cells (Boylan et al., 1993; Plassat et al., 2000). More importantly, they demonstrate that ST1926 and CD437 activated RARγ in a natural cellular context and behaved like classic retinoids at the concentration considered.

ST1926 and CD437 Induce Growth Arrest and Cell Death via a RARγ-Independent Mechanism. We evaluated whether the RARγ-dependent cytodifferentiation induced by the two RRMs was accompanied by growth inhibition. As documented by Fig. 2B, the action of ST1926 and CD437 could be divided in two phases. In fact, within the first 48 h, both compounds blocked the growth of F9-WT and F9γ−/− cells. At first, growth inhibition was not accompanied by a loss in cell viability, which was always above 80%, as observed in the case of control cultures (data not shown). After 2 days of treatment, a progressive and similar decrease in viability was evident in both cell lines. Contrary to what was observed in the case of the two RRMs, equimolar concentrations of ATRA induced only a delay in the growth of F9-WT and F9γ−/− cells and no significant cytotoxicity at any of the time points considered. As shown in Fig. 2C, increasing the concentration of ST1926 and CD437 to 2 μM caused a dose-dependent decrease in the number of viable cells already evident at 48 h. In these conditions, ST1926 and CD437 reduced the viability of F9-WT cells from 88 ± 1% (mean ± S.D., $n = 3$) to 66 ± 2 and 63 ± 6 at 0.5 μM, 29 ± 4% and 41 ± 10% at 1 μM, as well as 12 ± 4% and 6 ± 2% at 2 μM. Even at these relatively high concentrations, the cytotoxic effect of the two compounds did not correlate with RARγ expression. In fact, not only F9-WT and F9γ−/− cells but also F9γ51 cells showed very similar responses to the cytotoxic action of ST1926 and CD437. It is noteworthy that even the highest concentrations of ATRA (1 and 2 μM), though producing a growth inhibitory effect (Fig. 2C), continued to be devoid of significant cytotoxic activity on any of the cell lines considered. In fact in all cases, cell viability did not differ significantly from control conditions (data not shown). Overall, our results indicate that, in the case of both the RRMs and ATRA, growth inhibition was dissociated from the induced cytodifferentiating action. More importantly, they demonstrate that the observed growth inhibitory effects of ST1926 or CD437 and ATRA were intrinsically different. ATRA showed a pure antiproliferative action, whereas the activity of the other two compounds on F9 cell growth involved both an antiproliferative and a cytotoxic component.

ST1926 and CD437 Induce a G_2/M Arrest of the Cell Cycle. The cell cycle perturbations afforded by low concentrations (0.1 μM) of the two RRMs and ATRA were determined within the first 24 h of treatment. These experimental conditions were designed to avoid interferences caused by cytotoxicity. Figure 3 shows FACS profiles, along with the corresponding quantitative results, of F9-WT and F9γ−/− cells treated for 12 and 24 h with the three compounds. The overall picture of the cell cycle perturbations afforded by
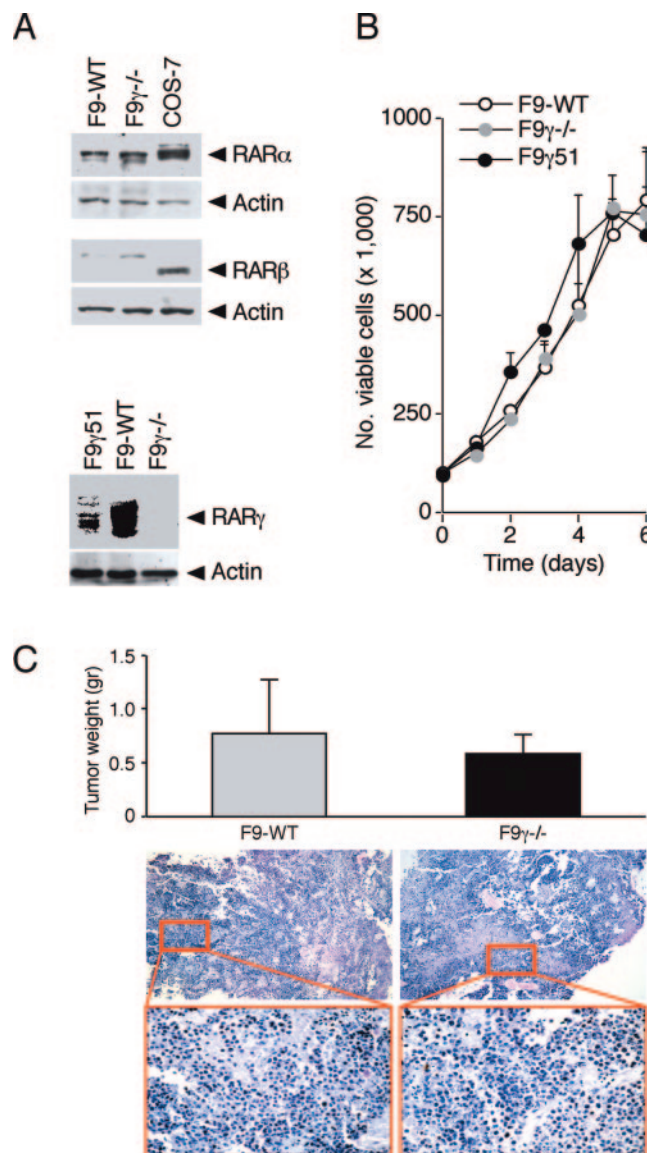
ST1926 and CD437 was similar in both F9 lines. The two compounds caused a rapid depletion of the G$_1$ compartment that was already evident at 12 h. This was accompanied by an expansion of the S and/or G$_2$/M phase. The results obtained with ATRA were significantly different. Despite a slowed progression along the cell cycle, indicated by an increase in the S phase at 24 h, ATRA caused no accumulation in G$_2$/M in either F9-WT or F9γ−/− cells. The expected accumulation in G$_1$, as demonstrated in previous reports (Li et al., 2004), was observed at later time points (3–4 days, data not shown). It was clear that ST1926/CD437 and ATRA blocked the cells in two distinct phases of the cycle, demonstrating that the cellular mechanisms activated were different. Thus, our results support the concept that a classic retinoid dependent response was not at the basis of the early growth arrest afforded by RRMs.

ST1926 and CD437 Were Characterized by an Apoptotic Action That Did Not Require RARγ. As shown in Fig. 4A, treatment of F9-WT, F9γ−/−, and F9γ51 cells with ST1926 for 24 h induced morphological changes characteristic of apoptosis in a dose-dependent manner and

regardless of RARγ expression. This was accompanied by the appearance of early apoptotic markers, such as annexin V binding to the plasma membrane (Fig. 4B) and caspase-3 activation (Fig. 4C). The fraction of viable (annexin V and PI negative, AV−/PI−), early apoptotic (AV+/PI−), late apoptotic (AV+/PI+), and necrotic (AV−/PI+) cells present in F9-WT and F9γ−/− cultures was evaluated by flow cytometry, after treatment with ST1926 or ATRA (0.5 μM) for 24 h. Fig. 4B, left, shows typical FACS scatter plots obtained upon challenge of F9 cells with vehicle or ST1926. A summary of the quantitative data is presented in bar graphs. In both F9-WT and F9γ−/− cultures, ST1926 caused a similar increase in the proportion of early and late apoptotic cells, leaving the number of necrotic cells basically unaltered. This was mirrored by a proportional decrease in the number of viable cells in ST1926 treated F9-WT and F9γ−/− cultures. Exposure of F9γ−/− and F9-WT cells to 0.5 μM ST1926 or CD437 for 24 h resulted in a similar activation of the early apoptotic marker, caspase-3, as measured by hydrolysis of the DEVD-amc substrate (Fig. 4C). Taken together, our re-
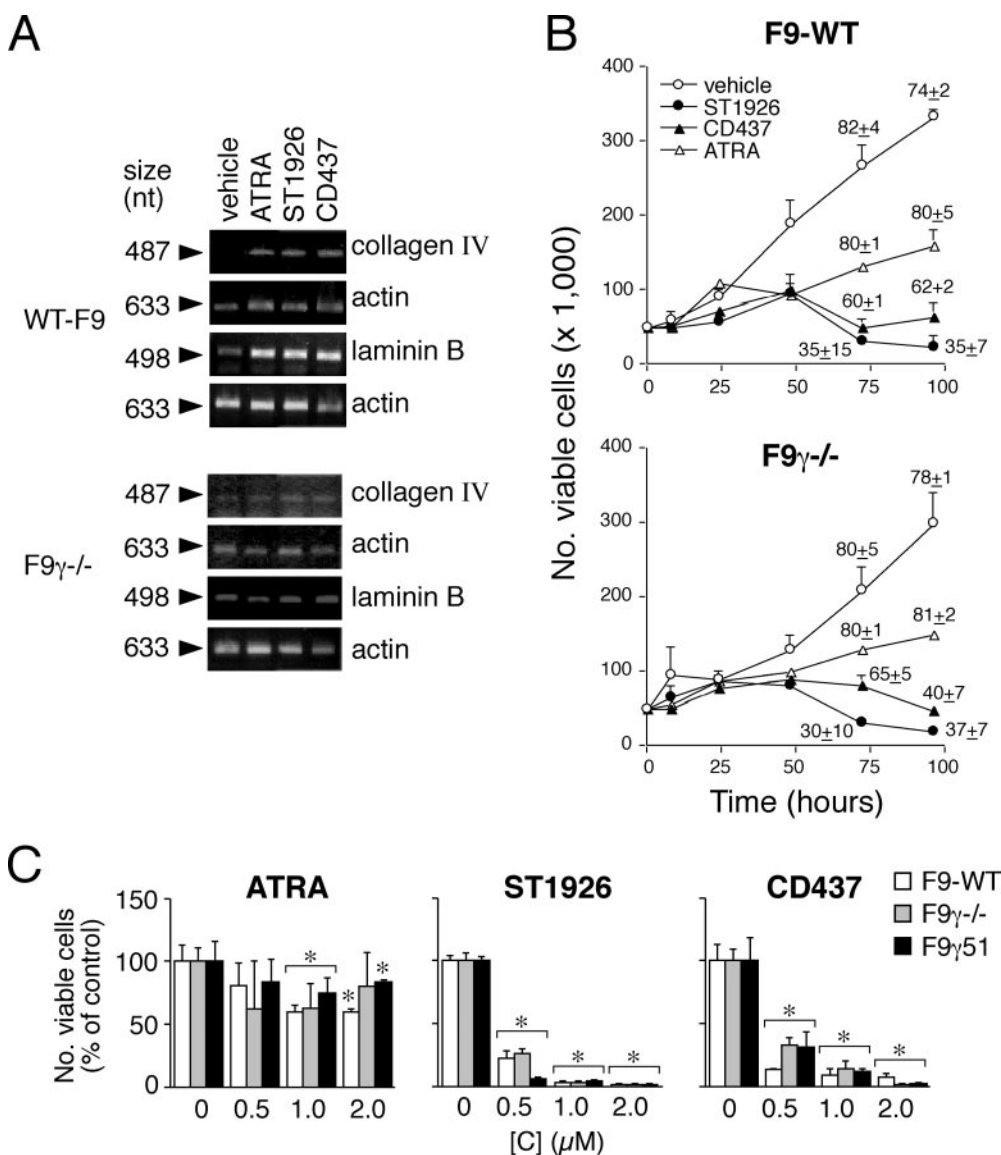

Fig. 2. Cytodifferentiating, antiproliferative, and cytotoxic activities of RRMs and ATRA in F9-WT, F9γ−/−, and F9γ51 cell lines. A, total RNA was extracted from the indicated cell lines after incubation for 48 h with vehicle, 0.1 μM ATRA, ST1926, and CD437. An equivalent amount of RNA (1 μg) was subjected to RT-PCR with couples of amplimers specific for collagen type IV, laminin B1 subunit 1, and actin. PCR-amplified bands were electrophoresed in 1% agarose gels and stained with ethidium bromide. The size of the amplified bands is indicated on the left. B, growth curves of F9 cells treated with low concentrations of RRMs and ATRA. F9-WT and F9γ−/− cells were treated with vehicle (DMSO) and the same concentration (0.1 μM) of ST1926, CD437, or ATRA for different lengths of time. The number of cells was determined after staining with erythrosine. During the first 48 h of treatment, the viability of cells is the same in all experimental groups (> 80%) and the corresponding values are not indicated. The viability observed for each experimental group is shown (mean ± S.D., n = 3) in correspondence, with each point of the graph starting from the 72-h time point. C, the indicated cell lines were treated with vehicle (DMSO), ATRA or the indicated RRMs for 48 h. At the end of the treatment, adhering cells were harvested and counted after staining with erythrosin. The values are the mean ± S.D. of three replicate cell cultures. ∗, significantly lower than the relative control value (p < 0.01 according to the Student's t test).

sults indicate that apoptosis was the main modality of the observed RRM-induced cytotoxic effect.

Equimolar concentrations of ATRA exerted no significant effect on the proportion of live or apoptotic cells relative to control conditions (Fig. 4B). The apoptosis markers considered were negative in all types of F9 cells treated with up to 1 μM ATRA and for up to 6 days. Indeed, F9γ−/− cell cultures exposed to 1 μM ATRA for 6 days contained 90 ± 1% live, 4 ± 1% early apoptotic, 1 ± 0.2% late apoptotic, and 4 ± 1% necrotic cells, compared with 92 ± 1% live, 5 ± 1% early apoptotic, 1 ± 0.1% late apoptotic and 3 ± 1% necrotic cells in the corresponding vehicle-treated cell cultures. Similar results were obtained in F9-WT cells (data not shown). Thus, in conditions of complete cell-kill by ST1926 and CD437, ATRA did not show apoptotic or cytotoxic activity. The data indicate that RARγ expression neither mediated nor modulated RRM-induced programmed cell death. In addition, they suggest that activation of the retinoic acid nuclear receptor pathway is unlikely to be significant for the apoptotic process activated by RRMs.

The Apoptotic Response of F9 Cells to RRMs Involved an Early Rise in Cytosolic Calcium. One of the earliest effects activated by RRMs in the NB4 leukemia cell line was is an increase in cytosolic calcium ions (Garattini et al., 2004a). We proposed that the phenomenon is at the basis of the apoptotic process activated in this cell line. To establish whether perturbations in the homeostasis of calcium are a general phenomenon, we performed a number of experiments in the F9 model.

In a first set of experiments (Fig. 5A), the amounts of intracellular calcium were determined semiquantitatively in single F9-WT cells grown as monolayers and preloaded with the calcium indicator Fluo3-AM. Treatment of F9-WT cells for up to one h with ST1926, but not vehicle (data not shown), resulted in a significant and time-dependent increase of intracellular calcium. This effect is evident in the majority of ST1926 treated cells. Similar results were obtained in F9γ−/− cells (data not shown). To get quantitative information on the phenomenon, FURA-2 was measured continuously on suspensions of F9-WT and F9γ−/− cells after addition of ST1926 or CD437 (Fig. 5B). Treatment with the two RRMs leads to an immediate increase in the cytosolic levels of calcium with very similar time courses.

The time dependence values for the elevation of FURA-2 fluorescence induced by ST1926 and CD437 in the two cell lines are very similar. At equimolar concentrations, ATRA (Fig. 5B, right) and inactive ST1926 congeners (data not shown) exerted no significant action on calcium homeostasis. Our data demonstrate that RRMs induced a rapid and long-lasting elevation of cytosolic calcium that is independent of the adherence to an extracellular substratum. Furthermore, they suggest that calcium mobilization represents an upstream event in the biochemical cascade activated by ST1926 and CD437 in F9 cells. In particular, RRM-dependent increases in cytosolic calcium preceded the appearance of any sign of apoptosis. As documented by Fig. 5C, the intracellular calcium chelator BAPTA (10 and 50 μM) suppressed the elevation of calcium afforded by ST1926 or CD437 in both cell lines. Figure 5D demonstrates that BAPTA (10 μM) blocked the RRM-dependent caspase-3 activation observed in F9γ−/− and F9-WT cells. These results indicate a central role for calcium, even in the case of a transcription and protein synthesis-dependent process of apoptosis like the one activated by RRMs in F9 cells.

Comparison of the Expression Profiles Associated with ST1926 and ATRA in F9-WT and F9γ−/− Cells Indicates Activation of Retinoid-Dependent and -Independent Pathways by RRMs. F9-WT and F9γ−/− cells were used to compare perturbations of the transcriptome induced by equimolar concentrations of ST1926 and ATRA. With this type of experiment, we aimed at gathering information on the molecular mechanisms underlying the action of ST1926. In particular, we intended to identify the gene profiles associated with the retinoid-dependent and -independent components of the RRM action. Furthermore, we wanted to establish the fraction of genes whose expression is controlled or modulated by RARγ activation.

As shown in Fig. 6A, treatment of F9-WT and F9γ−/− cells with ST1926 or ATRA (0.5 μM) for 10 h results in a significant up- or down-regulation of 2523 probes (2296 genes) ($p < 0.0001$ after two-way ANOVA for any of the two factors, cell line or treatment). A total of 903 probes (847 genes) has regulation patterns relevant to the study and can be classified in nine groups after Pavlidis template matching (Pavlidis and Noble, 2001) and hierarchical clustering (Fig. 6 and Fig. 7). A complete list of these genes and
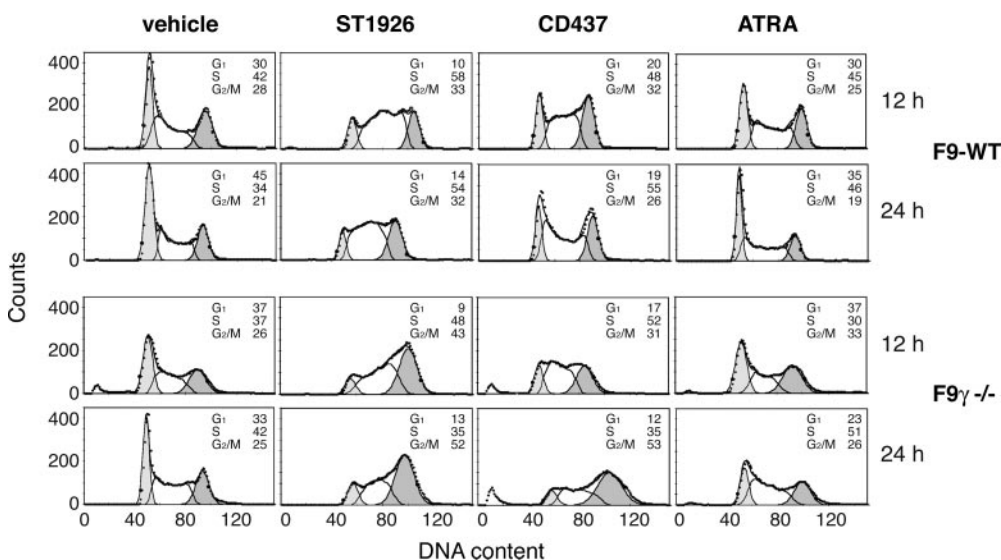
Fig. 3. Effects of RRMs and ATRA on the cell cycle phases of F9-WT and F9γ−/− cells. Representative FACS profiles of cells treated with 0.1 μM ST1926, CD437, and ATRA for 12 and 24 h. FACS analysis was performed after DNA staining with propidium iodide. The graphs show the experimental profile (dotted line) and the gaussian fitting (G₁ phase, light gray peaks; S phase, "empty" curves; G₂/M phase dark gray peaks; sum of the fitted curves, solid line). The percentage of cells present in the G₁, S, and G₂/M phases of the cycle is indicated. The data shown are representative of three experiments giving similar results.

their functional classification (using Ease; http://david.niaid.nih.gov/david/ease1.html) is presented in Supplementary Table 2. The diagram illustrates the number of genes falling in the various classes defined. Of the 178 probes under the control of ATRA (Fig. 6B, groups 1–6), 101 (57%) were regulated in a similar manner by ST1926

(groups 1–3). This supports the concept that the RRM is a bona fide retinoid and activates a substantial fraction of the same genetic program controlled by ATRA. However, our results also demonstrated that ST1926 regulated a much larger set of genes than ATRA in both F9-WT and F9γ−/− cells (826 versus 178; Fig. 6A). This indicates a major contribution of retinoid-inde-
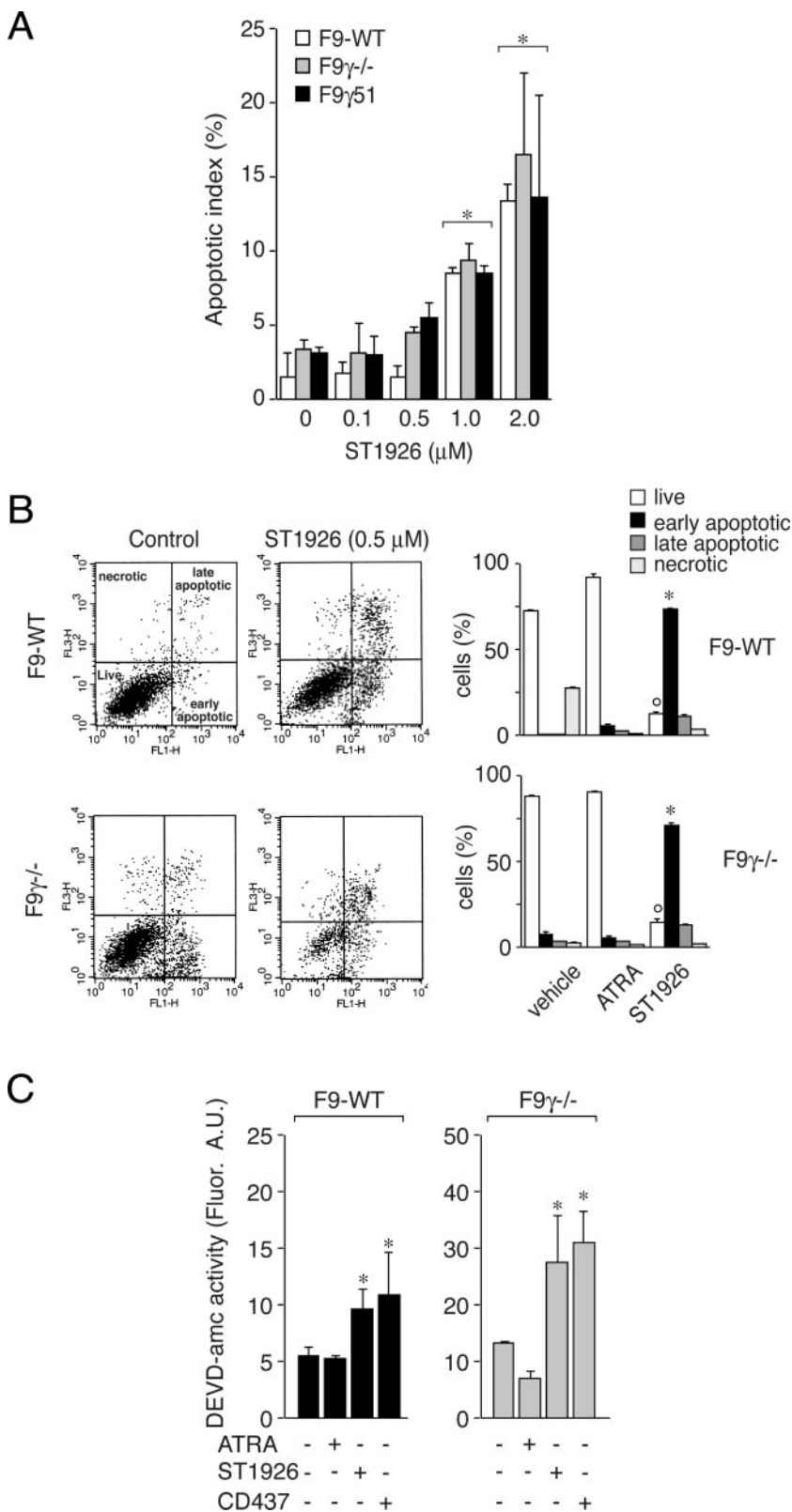

Fig. 4. Apoptosis and caspase activation of RRMs and ATRA in F9-WT and F9γ−/− cell lines. A, F9-WT and F9γ−/− cell lines were treated for 24 h with the indicated concentrations of ST1926. At the end of the treatment, adhering cells were scored for the number of fragmented nuclei (apoptotic index) after staining with 4,6 diamidino-2-phenylindole. Each value is the mean ± S.D. of three replicate cell cultures. ∗, significantly higher than the relative control value ($p < 0.01$ according to the Student's t test). B, left, shows representative FACS analyses of substrate adhering F9-WT and F9γ−/− cells treated for 24 h with vehicle (DMSO) or ST1926 (0.5 μM). Cells were stained with PI (vertical axis) and a fluorescein-conjugated antibody directed against annexin V (AV) (horizontal axis). AV−/PI− (lower left quadrant), AV−/PI+ (upper left quadrant), AV+/PI− (lower right quadrant), and AV+/PI+ (upper right quadrant) cells indicate live, necrotic, early apoptotic, and late apoptotic cells, respectively. Bar graphs of the quantitative results obtained on F9-WT and F9γ−/− cells treated for the indicated amounts of time with 0.5 μM ST1926 or ATRA are shown on the right. The results are the mean ± S.D. of three replicate cell cultures and were obtained after quantitation of the results shown by FACS analyses similar to those presented. Significantly higher (∗) or lower (°) than the relative control value ($p < 0.01$ according to the Student's t test). C, F9-WT and F9γ−/− cells were treated with 0.5 μM ATRA, ST1926, and CD437 for 24 h. At the end of the treatment, DEVD-amc hydrolytic activity was measured on cell extracts and expressed in fluorescence arbitrary units (A.U.). Each value is the mean ± S.D. of three replicate cell cultures. ∗, significantly higher than the relative control value ($p < 0.01$ according to the Student's t test).

pendent pathways to the early action exerted by ST1926 on the F9 transcriptome.

Genes Regulated Concomitantly by ST1926 and ATRA Defined Classic Retinoid Responses. Group 1 includes target genes up- or down-regulated concomitantly by ST1926 and ATRA in both F9-WT and F9γ−/− cells (Fig. 6B). This group consisted of genes possibly modulated by ligand-induced activation of RARα/RARβ. Among the genes whose expression was diminished, Myc and the DNA methyltransferase 3B stand out. Myc is a gene down-regulated by retinoids in different cellular contexts and is known to control progression from the G_1 to the S phase of the cycle. Myc down-regulation may play a role in the cell cycle arrest triggered by ATRA in G_1 but is unlikely to be a major determinant of the G_2/M arrest observed in the case of ST1926. DNA methyl transferases are associated with gene silencing, and their inhibition has been implicated in the gene activation effects triggered by classic retinoids (Fazi et al., 2005).

The cluster of genes up- or down-regulated by ST1926 and ATRA in F9-WT cells preferentially (Fig. 6B, group 2) was

likely to be under the control of ligand-activated RARγ. Homeobox A5 and iroquois-related-homeobox 2 belong to this group, suggesting a particular significance for the process of primitive endodermal maturation induced by ST1926 and ATRA. Indeed, homeotic genes are well known retinoic acid targets and are implicated in morphogenesis and organogenesis (Deschamps and van Nes, 2005). Several other members of this family were noticeably induced preferentially by ATRA in a RARγ-dependent fashion (Fig. 6B, group 5). Homeobox gene A1 (*HOXA1*) was the only HOX gene induced specifically by ATRA not only in F9-WT but also in F9γ−/− cells (Fig. 6B, group 4). However, the basal levels of HOXA1 expression were much higher in the former than in the latter cell line (Miamexpress; accession number E-MEXP-361), suggesting RARγ independence in the case of induced expression and possible RARγ dependence in the case of basal expression.

The molecular signature associated with ST1926 and ATRA in F9γ−/− cells (Fig. 6B, group 3) was of unknown significance and consisted of 11 genes. The sole gene up-
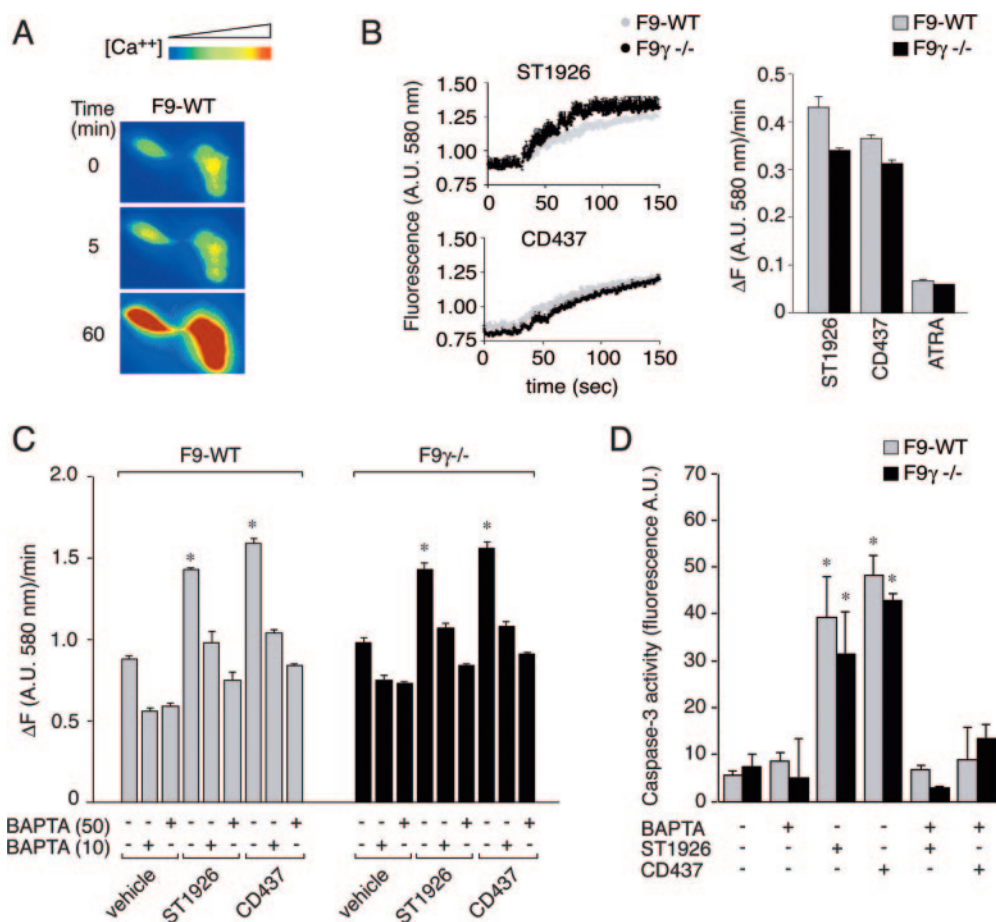

Fig. 5. Effect of ATRA, ST1926, and congeners on cytosolic calcium homeostasis. A, F9-WT and F9γ−/− cells were seeded on appropriately treated glass slides and loaded with the intracellular calcium indicator Fluo3-AM. Loaded cells were treated for up to 1 h with ST1926 (1 μM) and the amounts of Fluo3-AM derived fluorescence were measured continuously at the single cell level. The picture illustrates the levels of cytosolic calcium accumulation in two adjacent cells using pseudo-colors. B and C, FURA-2–loaded F9-WT and F9γ−/− cells were stimulated with the indicated compounds at a concentration of 1 μM and fluorescence measured continuously over the course of 2.5 min. B, left, shows continuous measurements, whereas C and B, right, show quantifications of the results, expressed as variation of fluorescence arbitrary units/time (ΔF/min) and calculated during the linear phase of calcium rise. In the case of the results shown in C, before addition of RRMs, cells were preincubated in the presence or absence of 10 and 50 μM BAPTA for 2 min. Each experimental value is the mean ± S.D. of three replicate cell cultures. *, significantly higher than the relative control value (p < 0.01 according to the Student's t test). D, DEVD-amc hydrolytic activity was measured in extracts of cells treated for 24 h with ST1926 (1 μM) or CD437 (1 μM) in the presence or absence of BAPTA (10 μM). The results are expressed in fluorescence arbitrary units (A.U.) and represent the mean ± S.D. of three replicate cell cultures. *, significantly higher than the relative control value (p < 0.01 according to the Student's t test).
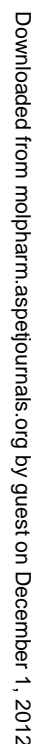
regulated in this group was the G protein α3, a polypeptide involved in G-protein signaling.

Genes Specifically Regulated by ST1926 Defined Nonretinoid-Associated Responses. The genes modulated by ST1926, and not by ATRA, in both F9-WT and F9γ−/− cells (Fig. 7, group 7) are likely to be relevant for the selective in vitro apoptotic action and G$_2$/M arrest triggered by the RRM. Consistent with this notion, 23 of the 355 up-regulated genes are proapoptotic or involved in the arrest of the cell cycle. For the same reason, 11 of the 163 down-regulated genes are positive modulators of cell growth. The list of proapoptotic genes includes elements of both the intrinsic and extrinsic pathways of programmed cell death, such as p73, caspase-3, members of the TNF receptor family, and TRAF4. As for TNF receptors, it is important to underscore that these proteins belong to the same family of the death receptors that plays a fundamental role in the extrinsic pathway of apoptosis. CD437 has been proposed to exert its apoptotic action through activation of autocrine or paracrine loops involving death receptors and corresponding ligands, such as the FAS and FAS-ligand couple (Sun et al., 2000b; Jin et al., 2005). In group 7, PERP, APAF1, and Bcl-2 binding component 3, are direct or indirect targets of p53. It is noteworthy that F9 teratocarcinoma cells are known to express wild-type p53 (Mayo and Berberich, 1996), which sensitizes other types of neoplastic cells to the action of RRMs (Sun et al., 1999). Given the importance of calcium in the process of apoptosis triggered by RRMs, the presence of 19 genes encoding polypeptides, such as protein phosphatase 1D and diacylglycerol kinase α, regulated by the cation, was of particular significance. The modulation of these genes might be the consequence of the early increase in calcium ions afforded by ST1926 and CD437. Group 7 contained a number of induced genes involved in DNA repair (four genes, six probes; Supplemental Table 1), suggesting that ST1926 may have DNA damaging activity (Garattini et al., 2004b).

Groups 8 and 9 consisted of genes modulated by ST1926, but not ATRA, in either F9-WT or F9γ−/− cells specifically. In F9γ−/− cells, treatment with ST1926 caused down-regulation of four genes involved in motility and angiogenesis and up-regulation of three genes responsible for cellular adhesion (Fig. 7, group 9). Conversely, the RRM induced the expression of two cell motility and angiogenesis genes (septin 2 and neuropilin) in F9-WT cells. Induction of group 8 gene products acting at the interface between the cell and the extracellular space, such as receptors of the platelet-derived growth factor or TNF family and BMP membrane bound

inhibitor (Supplemental Table 1), are also of particular interest. These observations indicate that ST1926 has RARγ-dependent effects on cellular processes other than proliferation, differentiation, and apoptosis.

ST1926 and CD437 Modulated the Same Type of Genes. The results obtained with whole-genome microarrays were validated and extended to CD437 for a selected number of genes. A first validation was conducted by semiquantitative agarose gel electrophoresis of the cDNA bands obtained by RT-PCR (Fig. 8A, left). For c-kit, c-myc, Notch Hom.3, and the homeo box A1 (*HOXA1*) gene, we also obtained quantitative results by Taqman real-time PCR (Fig. 8A, right). The experiments presented were totally independent of each other and of the ones used for the microarray analysis. The expression profile of all the genes considered was entirely consistent with what was observed with the microarray experiments. A small exception to this rule (1 of 10 genes, including *RARβ*; see below) is represented by c-kit, which shows induction by ST1926 (and CD437) also in F9γ−/− cells. This may be because the primers used for the RT-PCR and Taqman real-time PCR analyses are targeted against regions of the transcripts that are different from those represented by the corresponding microarray probes. Consistent with the primary microarray data, the Taqman data demonstrate that the constitutive levels of the HOXA1 transcript are lower in the F9γ−/− than in F9-WT cells. It is noteworthy that all these genes were regulated by CD437 in a fashion similar to that of ST1926, suggesting that the two compounds activate a very similar genetic program. This further supports the concept that ST1926 and CD437 belong to the same functional family of compounds (Garattini et al., 2004a).

RARβ belonged to the group of genes induced by ATRA more than ST1926 in both F9-WT and F9γ−/− cells (group 4). As a whole, the RT-PCR data (Fig. 8B) confirmed that the receptor was induced more efficiently by ATRA than by RRMs in F9γ−/− cells. However, this differential effect was not observed in F9-WT cells, also because of the lower basal levels of the transcript in this cell line. Although quantitative differences in the induction of RARβ by ATRA and ST1926 or CD437 were observed in F9-WT and F9γ−/− cells, the finding is in agreement with previous results indicating that RARβ2 can be up-regulated by multiple RAR isoforms in a redundant fashion (Rochette-Egly and Chambon, 2001). It is noteworthy that RARβ was the only retinoid receptor whose expression was modulated by RRMs or ATRA in F9 cells. In fact, ST1926, CD437, and ATRA did not affect the basal level

Fig. 6. Gene expression profiling: general results and classic retinoid responses. F9-WT and F9γ−/− cells were treated with vehicle (DMSO), ATRA (0.5 μM), or ST1926 (0.5 μM) for 10 h. Poly(A+) RNA was isolated from three separate culture flasks and pooled. In the first experimental replicate (leftmost lane of each experimental group), vehicle RNA was labeled with the fluorochrome Cy3, whereas ATRA- or ST1926-RNA was labeled with Cy5. In the second experimental replicate (rightmost lane of each experimental group), fluorochromes were swapped; i.e., vehicle-RNA was labeled with Cy5, whereas ATRA- or ST1926-RNA was labeled with Cy3. Cy3 and Cy5 RNAs were mixed in equimolar amounts and hybridized to oligonucleotide microarrays. After filtering the data for significant changes using two-way ANOVA (*p* < 0.0001), groups of genes with interesting regulation pattern were selected after hierarchical clustering (group 1) or Pavlidis template matching (all other groups). A, the scheme represents the number of probes up-regulated (red arrow) or down-regulated (green arrow) in the various experimental conditions. Probes are grouped according to the pattern of expression. B, the genes regulated by ST1926 and ATRA concordantly in both F9-WT and in F9γ−/− cells are presented in group 1. Group 2 contains genes controlled by ST1926 and ATRA in F9-WT cells preferentially. Group 3 consists of genes regulated by ST1926 and ATRA in F9γ−/− cells. Group 4 represents genes modulated by ST1926 alone in both F9-WT and in F9γ−/− cells. The genes whose expression is specifically modulated by ATRA in F9-WT and F9γ−/− exclusively are shown in groups 5 and 6, respectively. The values next to each node indicate the number of probes present in the corresponding cluster (green, down-regulated genes; red, up-regulated genes). Color scale refers to log2Ratios of treated samples versus corresponding control samples. Duplicates correspond to swapped samples. A shortened description of each gene and the relative GenBank accession number is indicated. The list of the genes in all clusters, with the gene ontology classification and the quantitative changes is reported in Supplemental Table 1.

of expression of RARα, RARγ, or the three RXR isoforms (Fig. 8B, left).

In Vivo, the Antitumor Activity of RRMs Was Hindered by RARγ Expression in the Neoplastic Cell. The microarray results provide information on the possible molecular determinants of the RARγ-independent processes (growth inhibition and apoptosis) triggered by RRMs in F9

cell cultures. However, they also point to a set of RARγ-dependent alterations in genes controlling processes of potential significance for the antitumor activity of RRMs in vivo, such as cell adhesion, motility, angiogenesis, proteolysis, and tumor/host interactions. Indeed, the microarray results suggest that RRM antitumor activity might be higher in the absence of RARγ.
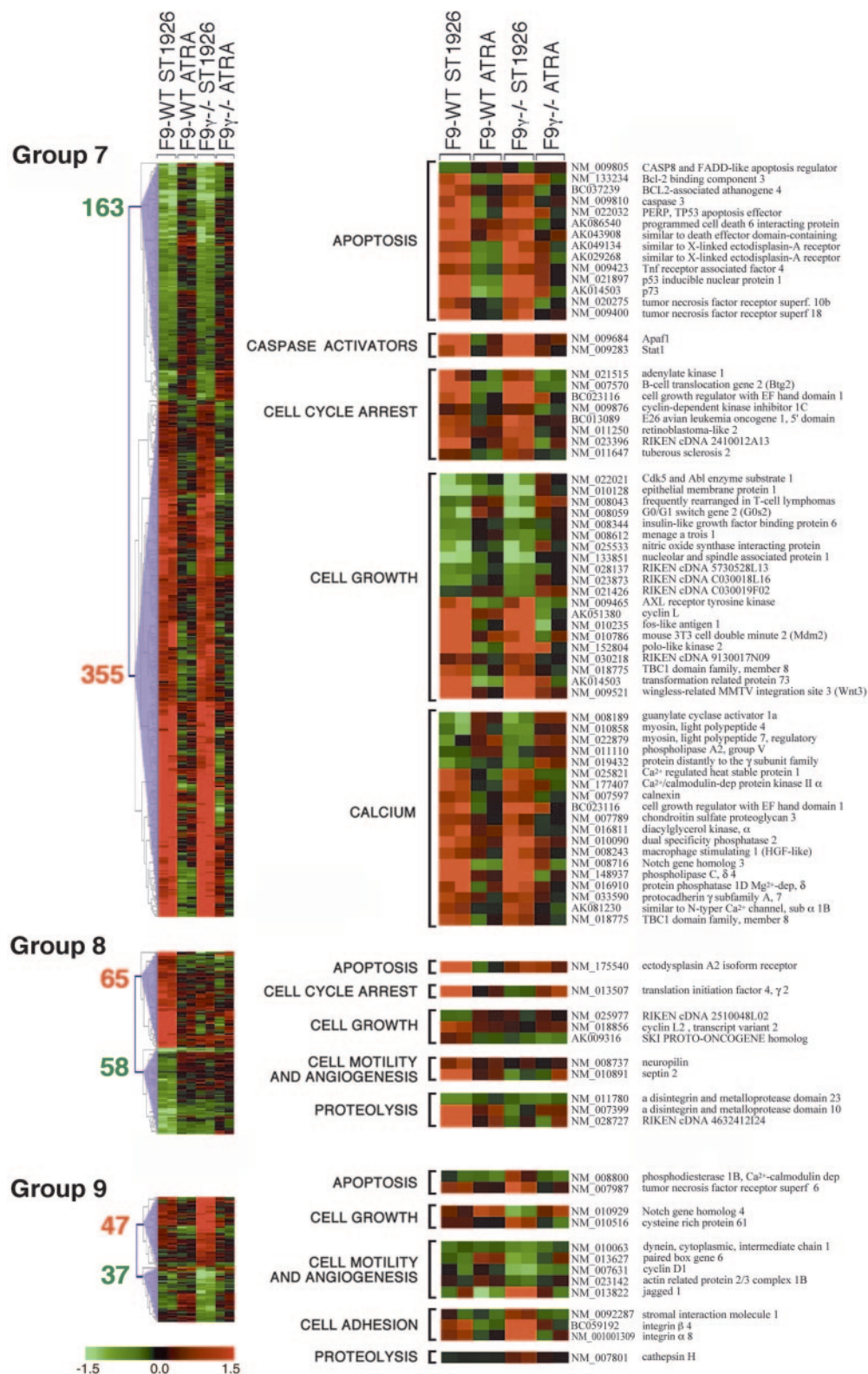
Fig. 7. Gene expression profiling: nonclassic retinoid responses. Left, hierarchical clustering of genes modulated preferentially by ST1926 in both F9-WT and F9γ−/− (group 7), F9-WT (group 8), or F9γ−/− (group 9) cells only. Data are organized and presented as in Fig. 8. The list of the genes in all clusters, with the gene ontology classification and the changes, is reported in Supplemental Table 1. Right, a selection of functionally interesting genes extracted from each group. Genes are classified according to the major area of functional interest.

The above hypothesis was tested directly in vivo, taking advantage of the fact that F9-WT and F9γ−/− grow as tumors in syngeneic mice (Fig. 1C). Figure 9A demonstrates that long-term intraperitoneal administration of ATRA at the maximal tolerated dose of 15 mg/kg did not alter the survival of either F9-WT or F9γ−/− tumor-bearing animals. The finding indicates that the ATRA-dependent antiproliferative and cytodifferentiation effects observed in cultures of F9 cells were not sufficient to translate into a therapeutic effect in vivo. In contrast, Fig. 9B demonstrates that oral administration of ST1926 (30 mg/kg) resulted in a significant increase in the median survival time of mice inoculated with both F9-WT and F9γ−/− cells. Consistent with our hypothesis, ST1926 was much more effective in F9γ−/− than in F9-WT tumor-bearing animals. Differential sensitivity of F9γ−/− and F9-WT tumors was independent of the administration route, in that a similar phenomenon was observed after i.p. treatment with ST1926 (Fig. 9C). Furthermore, the phenomenon was observed also in the case of the other RRM, CD437. Immunological responses do not seem to be at the basis of the observed differences in sensitivity between the F9γ−/− and F9-WT tumors. This is supported by the results obtained in the B- and T-cell–deficient SCID mouse (Fig. 9D). Even in this model, ST1926 and CD437 (i.p. administered) demonstrate a superior effect on mice bearing F9γ−/− tumors. Thus, our results demonstrate that RARγ expression hinders the response of F9 cells to the therapeutic activity of RRMs in vivo. More importantly, they suggest that the in vivo action of RRMs is not simply the result of a direct cytotoxic and growth inhibitory action on tumor cells and may involve effects on the processes of metastatization, angiogenesis, or interactions with the host environment.
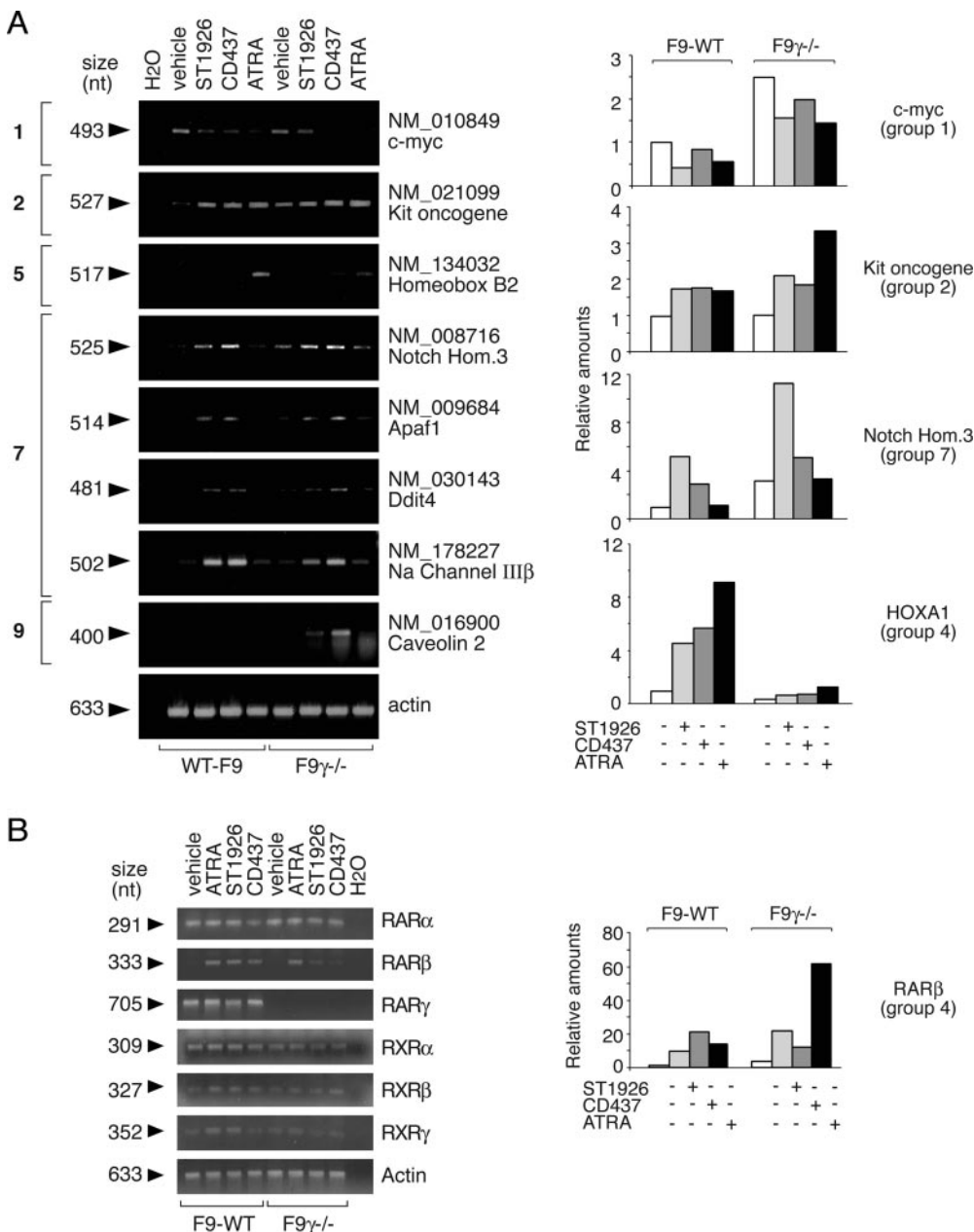

Fig. 8. PCR validation of the microarray results. A and B, total RNA was extracted from the indicated cell lines after incubation for 10 h with ATRA, ST1926, and CD437 (0.5 μM). Left, an equivalent amount of RNA (1 μg) was subjected to RT-PCR with couples of amplimers specific for the indicated genes. The PCR reactions were stopped between the 25th and 30th cycles according to the gene considered to ensure linear amplification ranges. PCR-amplified bands were electrophoresed in 1% agarose gels and stained with ethidium bromide. The size of the amplified bands (A and B) and the clusters (A) in which they were classified after microarray data analysis (Figs. 8 and 9) are indicated on the left. Right, real-time Taqman PCR of the indicated genes was performed using β-actin as an endogenous control. The data are expressed in fold-induction relative to vehicle treated F9-WT cells ($2^{-\Delta\Delta C_T}$). The results derive from two replicate CT determinations always with a variation coefficient lower than 2.5%.

Discussion

In this study, first we compared ST1926 and CD437 to ATRA for their ability to transactivate RARα, RARβ, and RARγ in COS-7 transfected cells. The data indicate that CD437 was a selective ligand of RARγ and a stronger agonist of the receptor than ATRA. ST1926 itself was a better RARγ transactivator than ATRA but lost RARγ selectivity. Both ST1926 and CD437 were poor RXR activators.

In F9 teratocarcinoma cells, we confirmed, in a native context, that ST1926 and CD437 were bona fide retinoids and had the potential to activate RARγ. As expected from classic retinoids with RARγ agonistic activity, low concentrations of the two RRMs were as effective as ATRA in inducing the cytodifferentiation of F9-WT but not F9γ-/- cells. The results obtained with whole-genome microarrays support the concept that ST1926 is endowed with classic retinoid activity.
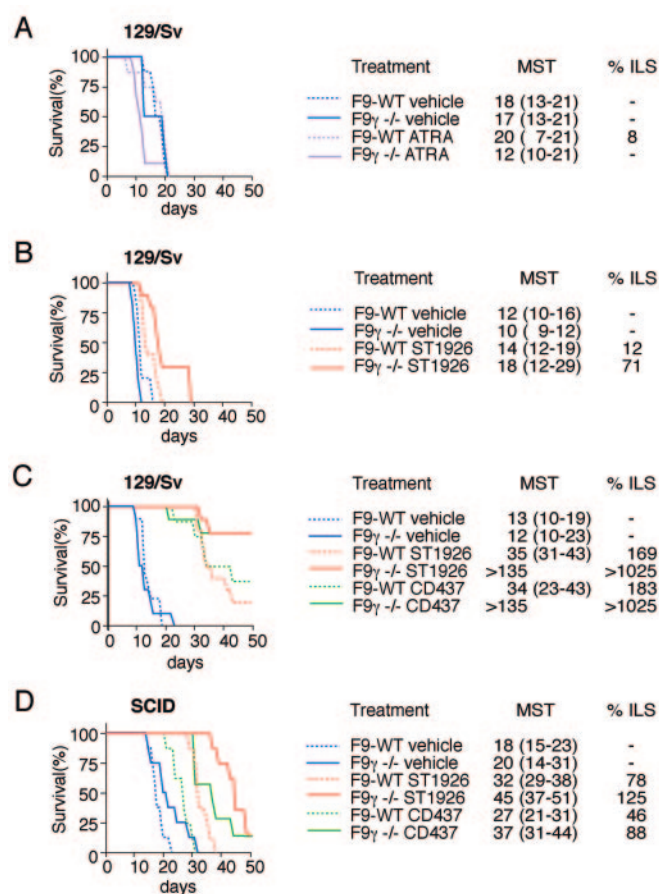

Fig. 9. In vivo effect of ST1926, CD437, and ATRA on the survival of animals transplanted with F9-WT and F9γ-/- tumors. F9-WT and F9γ-/- cells were inoculated (3×10^6/animal) i.p. into syngeneic 129/Sv (A–C) or SCID (D) mice (10 animals/experimental group). The graphs show Kaplan Meyer's survival curves. MST, median survival time expressed in days; the number in parentheses indicates the survival time range. %ILS, percentage increase in life span relative to the corresponding experimental group treated with vehicle. The value is calculated as follows: %ILS = (MST treated/MSTcontrol × 100) − 100. A, twelve hours after inoculation, animals were i.p. administered vehicle or ATRA (15 mg/kg), five times a week for 2 weeks. B, twelve hours after inoculation, animals were administered vehicle or ST1926 (30 mg/kg) orally, five times a week for 2 weeks. C, six hours after inoculation, animals were i.p. administered vehicle, ST1926, or CD437 (20 mg/kg), five times a week for 2 weeks. D, six hours after inoculation, SCID mice were i.p. administered vehicle ST1926 or CD437 (20 mg/kg) five times a week for 2 weeks.

ST1926 modulates the expression of a large proportion of the genes controlled by ATRA in F9-WT and F9γ-/- cells. A similar proportion of coregulated genes is observed in the responses specific for the F9-WT cellular context, where ATRA and RRM dependence is likely to be mediated by RARγ. These genes are of particular interest for the differentiation of teratocarcinoma cells along the parietal endoderm pathway.

The data obtained in the F9 model indicate that retinoid activity was unlikely to play a significant role in RRM-induced apoptosis, which is a primary determinant of ST1926 and CD437 antitumor activity. Indeed, the apoptotic action of RRMs is not shared by ATRA, strongly suggesting that programmed cell death is not a direct consequence of the retinoid-dependent cytodifferentiating effects as in NB4 leukemic cells (Giannì et al., 2000). Furthermore, unlike cytodifferentiation, apoptosis was independent of RARγ activation, as observed in F9-WT, F9γ-/-, and F9γ51 cells. Our results are consistent with the idea that ST1926 and CD437 activated not only the classic retinoid pathway but also a second signaling pathway. In cultures of F9 cells, the second pathway is prevalent and is at the basis of the apoptotic effect.

Similar to what we observed in NB4 myeloid leukemia cells (Garattini et al., 2004a), the earliest event associated with RRM-induced apoptosis in F9 cells is the elevation of cytosolic calcium. In NB4 cells, we demonstrated previously that calcium increases are not due to a net influx of the cation from the extracellular compartment and might be the result of RRM effects on the reuptake of the ion by the mitochondrion. Whatever the underlying mechanism, the rise in calcium is necessary for the programmed cell death activated by RRMs in NB4 and in F9 cells. In fact, in this last cell line, whereas ST1926 and CD437 were powerful calcium-mobilizing agents, ATRA and inactive RRMs were devoid of this activity. More importantly, chelation of intracellular calcium by BAPTA prevented ST1926-induced caspase activation, one of the hallmarks of apoptosis. Calcium mobilization was not influenced by RARγ, in that identical effects were observed in the F9-WT and F9γ-/- cell lines. Although the mobilization of calcium observed in RRM-treated F9 teratocarcinoma and NB4 cells is similar, the ensuing process of apoptosis is intrinsically different. In NB4 cells, apoptosis is very rapid and does not require gene expression or de novo protein synthesis. In contrast, the apoptotic response of F9 cells was slower and might therefore be dependent on gene transcription and protein synthesis. If this was indeed the case, genes relevant for the RRM-dependent apoptosis in F9 cells must be sought for among the large number of probes identified as specific and RARγ-independent targets of ST1926 (the genes controlled by ST1926, but not ATRA, in both F9-WT and F9γ-/- cells). This set of genes is of particular significance and deserves evaluation as to calcium-dependent transcriptional modulation.

The overall antitumor effect of RRMs may be the result not only of apoptotic but also of antiproliferative effects. To establish this point, we conducted studies with low and comparable concentrations of ST1926 or CD437 and ATRA. Under these conditions, the process of apoptosis activated by the two RRMs was delayed and the antiproliferative effects could be studied in a relatively clean situation. Our data demonstrate that ST1926 and CD437 treatments were associated with an early S and G$_2$M cell cycle block in both F9-WT and
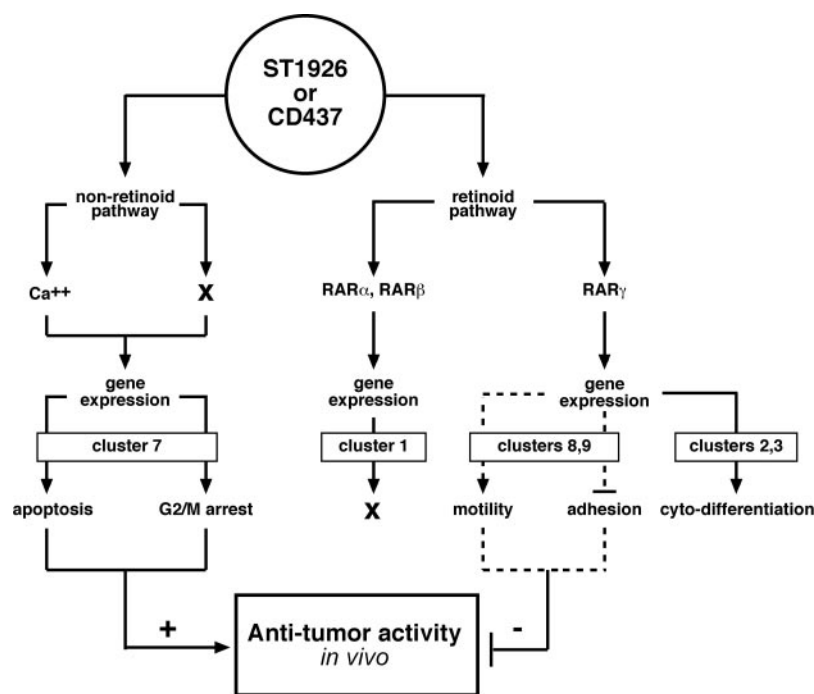
Fig. 10. Hypothetical scheme on the mechanisms underlying the pharmacological activity of RRMs in the F9 model. The scheme illustrates the various pathways activated by ST1926 and/or CD437 in F9 cells. Dashed lines indicate hypothetical processes activated by ST1926 based on the microarray data. The indication of clusters refers to the groups of genes determined with the microarray data analysis that may contain the determinants of the indicated processes.

F9γ−/− cells. The cell cycle block afforded by ATRA is different and consists of a G$_1$ arrest observed only after long exposures (3–4 days) (Li et al., 2004). The G$_1$ arrest caused by ATRA in both F9-WT and F9γ−/− cells suggests involvement of RARα and or RARβ. The assumption is in line with the observation that RARβ activation is a critical determinant of the growth arrest induced by ATRA in F9 cells (Faria et al., 1999; Zhuang et al., 2003).

Although RARγ is not a major determinant of RRMs' apoptotic and cytotoxic activity in vitro, the receptor seems to play an important role in the response of F9 tumor-bearing animals. Syngeneic and immunodeficient mice transplanted with F9γ−/− cells are more sensitive to RRMs than the corresponding counterparts inoculated with F9-WT cells. The phenomenon is not explained by differences in basal growth, in that the F9-WT and F9γ−/− untreated tumors grow in a similar fashion, show the same histological appearance, and are lethal to animals in approximately the same amount of time. Furthermore, the phenomenon is unlikely to reflect clonal variability between the F9-WT and F9γ−/− cells. In fact, animals transplanted with the two cell lines are equally insensitive to ATRA, whereas they respond equally well to intraperitoneal injection of other chemotherapeutic agents, such as cisplatin (M. M. Barzago and E. Garattini, unpublished observations). Although originally unexpected, this increased sensitivity may find an explanation in the profile of genes selectively modulated by ST1926 in either F9-WT or F9γ−/−. In fact, the cell type-specific effects observed on a number of genes controlling cell motility and angiogenic responses suggest relevance for the processes of invasion and metastasis. Overall, our data indicate that RARγ expression modulates some aspects of the host/tumor interaction unrelated to immune responses.

Figure 10 provides a summary and a rational interpretation of our observations. RRMs activated two distinct pathways in F9 cells. We defined as nonretinoid the actions exerted by ST1926 (and CD437) that were not shared by ATRA and that were likely to involve mechanisms unrelated to retinoic receptor activation. The nonretinoid pathway leads to G$_2$/M cell cycle arrest and apoptosis, which is mediated by a perturbation of calcium homeostasis. These two processes are likely to mediate a large proportion of the in vivo antitumor activity of both ST1926 and CD437. Although RARα and RARβ contribute to the genomic effects induced by ST1926 in F9 cells, activation of the two receptors does not seem to play a significant role in the overall antitumor activity of ST1926 and CD437 as well. Activation of RARγ by RRMs leads to cytodifferentiation; however, this phenomenon is unlikely to have any significance for the in vivo antineoplastic action of these compounds. In contrast, RARγ seems to have an important modulatory and negative role on the response to RRMs in vivo, perhaps by acting on genes involved in cell motility and adhesion.

In conclusion, the data presented provide the foundation for future studies aimed to define the functional relevance of the numerous genes modulated by RRMs. Our results also have far-reaching implications at the clinical level, in that they may orient the choice of target tumors. Indeed, if RARγ-related resistance is not limited to the F9 model, tumors with low or undetectable levels of the receptor would represent the primary targets against which to test ST1926 in phase II clinical trials. Finally, the genome-wide microarray data are a useful resource to design rational combinations of RRMs and other chemotherapeutics.

References

Altucci L and Gronemeyer H (2001) The promise of retinoids to fight against cancer. *Nat Rev Cancer* **1:**181–193.

Boylan JF, Lohnes D, Taneja R, Chambon P, and Gudas LJ (1993) Loss of retinoic acid receptor gamma function in F9 cells by gene disruption results in aberrant Hoxa-1 expression and differentiation upon retinoic acid treatment. *Proc Natl Acad Sci USA* **90:**9601–9605.

Bour G, Plassat JL, Bauer A, Lalavee S, and Rochette-Egly C (2005) Vinexin beta interacts with the non-phosphorylated AF-1 domain of retinoid receptor γ (RARγ) and represses RARγ-mediated transcription. *J Biol Chem* **280:**17027–17037.

Cao X, Liu W, Lin F. Li H, Kolluri SK, Lin B, Han YH, Dawson MI, Zhang XK (2004) Retinoid X receptor regulates Nur77/TR3-dependent apoptosis by modulating its nuclear export and mitochondrial targeting. *Mol Cell Biol* **24:**9705–9725.

Chun KH, Pfahl M, and Lotan R (2005) Induction of apoptosis by the synthetic retinoid MX3350–1 through extrinsic and intrinsic pathways in head and neck squamous carcinoma cells. *Oncogene* **24:**3669–3677.

Cincinelli R, Dallavalle S, Merlini L, Penco S, Pisano C, Carminati P, Giannini G, Vesci L, Gaetano C, Illy B, et al. (2003) A novel atypical retinoid endowed with proapoptotic and antitumor activity. *J Med Chem* **46:**909–912.

Dawson MI, Hobbs PD, Peterson VJ, Leid M, Lange CW, Feng KC, Chen Gq, Gu J, Li H, Kolluri SK, et al. (2001) Apoptosis induction in cancer cells by a novel analogue of 6-[3-(1-adamantyl)-4-hydroxyphenyl]-2-naphthalenecarboxylic acid lacking retinoid receptor transcriptional activation activity. *Cancer Res* **61:**4723–4730.

Delescluse C, Cavey MT, Martin B, Bernard BA, Reichert U, Maignan J, Darmon M, and Shroot B (1991) Selective high affinity retinoic acid receptor α or β-γ ligands. *Mol Pharmacol* **40:**556–562.

Deschamps J and van Nes J (2005) Developmental regulation of the Hox genes during axial morphogenesis in the mouse. *Development* **132:**2931–2942.

Faria TN, Mendelsohn C, Chambon P, and Gudas LJ (1999) The targeted disruption of both alleles of RARβ₂ in F9 cells results in the loss of retinoic acid-associated growth arrest. *J Biol Chem* **274:**26783–26788.

Fazi F, Travaglini L, Carotti D, Palitti F, Diverio D, Alcalay M, McNamara S, Miller WH Jr, Lo Coco F, Pelicci PG, et al. (2005) Retinoic acid targets DNA-methyltransferases and histone deacetylases during APL blast differentiation in vitro and in vivo. *Oncogene* **24:**1820–1830.

Garattini E, Giannì M, and Terao M (2004a) Retinoid related molecules an emerging class of apoptotic agents with promising therapeutic potential in oncology: pharmacological activity and mechanisms of action. *Curr Pharm Des* **10:**433–448.

Garattini E, Parrella E, Diomede L, Giannì M, Kalac Y, Merlini L, Simoni D, Zanier R, Ferrara FF, Chiarucci I, et al. (2004b) ST1926, a novel and orally active retinoid-related molecule inducing apoptosis in myeloid leukemia cells: modulation of intracellular calcium homeostasis. *Blood* **103:**194–207.

Garattini E and Terao M (2004) Atypical retinoids: an expanding series of anti-leukemia and anti-cancer agents endowed with selective apoptotic activity. *J Chemother* **16:**70–73.

Giannì M, Ponzanelli I, Mologni L, Reichert U, Rambaldi A, Terao M, and Garattini E (2000) Retinoid-dependent growth inhibition, differentiation and apoptosis in acute promyelocytic leukemia cells. Expression and activation of caspases. *Cell Death Differ* **7:**447–460.

Giannì M, Parrella E, Raska I Jr, Gaillard E, Nigro EA, Gaudon C, Garattini E, and Rochette-Egly C (2006) P38MAPK-dependent phosphorylation and degradation of SRC-3/AIB1 and RARalpha-mediated transcription. *EMBO (Eur Mol Biol Organ) J* **25:**739–751.

Jin F, Liu X, Zhou Z, Yue P, Lotan R, Khuri FR, Chung LW, and Sun SY (2005) Activation of nuclear factor-kappaB contributes to induction of death receptors and apoptosis by the synthetic retinoid CD437 in DU145 human prostate cancer cells. *Cancer Res* **65:**6354–6363.

Holmes WF, Dawson MI, Soprano RD, and Soprano KJ (2000) Induction of apoptosis in ovarian carcinoma cells by AHPN/CD437 is mediated by retinoic acid receptors. *J Cell Physiol* **185:**61–67.

Hsu CA, Rishi AK, Su-Li X, Gerald TM, Dawson MI, Schiffer C, Reichert U, Shroot B, Poirer GC, and Fontana JA (1997) Retinoid induced apoptosis in leukemia cells through a retinoic acid nuclear receptor-independent pathway. *Blood* **89:**4470–4479.

Kasturi J, Acharya R, and Ramanathan M (2003) An information theoretic approach for analyzing temporal patterns of gene expression. *Bioinformatics* **19:**449–458.

Knudsen S, Workman C, Sicheritz-Ponten T, and Friis C (2003) GenePublisher: automated analysis of DNA microarray data. *Nucleic Acids Res* **31:**3471–3476.

Li R, Faria TN, Boehm M, Nabel EG, and Gudas LJ (2004) Retinoic acid causes cell growth arrest and an increase in p27 in F9 wild type but not in F9 retinoic acid receptor beta2 knockout cells. *Exp Cell Res* **294:**290–300.

Lopez-Hernandez FJ, Ortiz MA, Bayon Y, and Piedrafita FJ (2004) Retinoid-related molecules require caspase 9 for the effective release of Smac and the rapid induction of apoptosis. *Cell Death Differ* **11:**154–164.

Mayo LD and Berberich SJ (1996) Wild-type p53 protein is unable to activate the mdm-2 gene during F9 cell differentiation. *Oncogene* **13:**2315–2321.

Marchetti P, Zamzami N, Joseph B, Schraen-Maschke S, Mereau-Richard C, Costantini P, Metivier D, Susin SA, Kroemer G, and Formstecher P (1999) The novel retinoid 6-[3-(1-adamantyl)-4-hydroxyphenyl]-2-naphtalene carboxylic acid can trigger apoptosis through a mitochondrial pathway independent of the nucleus. *Cancer Res* **59:**6257–6266.

Mologni L, Ponzanelli I, Bresciani F, Sardiello G, Bergamaschi D, Giannì M, Reichert U, Rambaldi A, Terao M, and Garattini E (1999) The novel synthetic retinoid 6-[3-adamantyl-4-hydroxyphenyl]-2-naphthalene carboxylic acid (CD437) causes apoptosis in acute promyelocytic leukemia cells through rapid activation of caspases. *Blood* **93:**1045–1061.

Pavlidis P and Noble WS (2001) Analysis of strain and regional variation in gene expression in mouse brain. *Genome Biol* **2:**RESEARCH0042.

Plassat J, Penna L, Chambon P, and Rochette-Egly C (2000) The conserved amphipatic alpha-helical core motif of RARgamma and RARalpha activating domains is indispensable for RA-induced differentiation of F9 cells. *J Cell Sci* **113:**2887–2895.

Ponzanelli I, Giannì M, Giavazzi R, Garofalo A, Nicoletti I, Reichert U, Erba E, Rambaldi A, Terao M, and Garattini E (2000) Isolation and characterization of an acute promyelocytic leukemia cell line selectively resistant to the novel antileukemic and apoptogenic retinoid 6-[3-adamantyl-4-hydroxyphenyl]-2-naphthalene carboxylic acid. *Blood* **95:**2672–2682.

Rishi AK, Zhang L, Boyanapalli M, Khadeer M, Inesi G, and Hussain A (2003) Identification and characterization of a cell cycle and apoptosis regulatory protein-1 as a novel mediator of apoptosis signaling by retinoid CD437. *J Biol Chem* **278:**33422–33435.

Rochette-Egly C and Chambon P (2001) F9 embryocarcinoma cells: a cell autonomous model to study the functional selectivity of RARs and RXRs in retinoid signaling. *Histol Histopathol* **16:**909–922.

Rochette-Egly C, Plassat JL, Taneja R, and Chambon P (2000) The AF-1 and AF-2 activating domains of retinoic acid receptor-alpha (RARalpha) and their phosphorylation are differentially involved in parietal endodermal differentiation of F9 cells and retinoid-induced expression of target genes. *Mol Endocrinol* **14:**1398–1410.

Saeed AI, Sharov V, White J, Li J, Liang W, Bhagabati N, Braisted J, Klapa M, Currier T, Thiagarajan M, et al. (2003) TM4: a free, open-source system for microarray data management and analysis. *Biotechniques* **34:**374–378.

Taneja R, Rochette-Egly C, Plassat JL, Penna L, Gaub MP, and Chambon P (1997) Phosphorylation of activation functions AF-1 and AF-2 of RAR alpha and RAR gamma is indispensable for differentiation of F9 cells upon retinoic acid and cAMP treatment. *EMBO (Eur Mol Biol Organ) J* **16:**6452–6465.

Sabichi AL, Xu H, Fischer S, Yang X, Steele VE, Kelloff GJ, Lotan R, and Clifford JL (2003) Retinoid receptor-dependent and independent biological activities of novel fenretinide analogues and metabolites. *Clin Cancer Res* **9:**4606–4613.

Sun SY, Yue P, Wu GS, El-Deiry WS, El-Deiry WS, Shroot B, Hong WK, and Lotan R (1999) Implication of p53 in growth arrest and apoptosis induced by the synthetic retinoid CD437 in human lung cancer cells. *Cancer Res* **59:**2829–2833.

Sun SY, Yue P, Chandraratna RA, Tesfaigzi Y, Hong WK, and Lotan R (2000a) Dual mechanisms of action of the retinoid CD437: nuclear retinoic acid receptor-mediated suppression of squamous differentiation and receptor-independent induction of apoptosis in UMSCC22B human head and neck squamous cell carcinoma cells. *Mol Pharmacol* **58:**508–514.

Sun SY, Yue P, Chen X, Hong WK, and Lotan R (2002) The synthetic retinoid CD437 selectively induces apoptosis in human lung cancer cells while sparing normal human lung epithelial cells. *Cancer Res* **62:**2430–2436.

Sun SY, Yue P, Hong WK, and Lotan R (2000b) Induction of Fas expression and augmentation of Fas/Fas ligand-mediated apoptosis by the synthetic retinoid CD437 in human lung cancer cells. *Cancer Res* **60:**6537–6543.

Ubezio P (1985) Microcomputer experience in analysis of flow cytometric DNA distributions. *Comput Programs Biomed* **19:**159–166.

Workman C, Jensen LJ, Jarmer H, Berka R, Gautier L, Nielser HB, Saxild HH, Nielsen C, Brunak S, and Knudsen S (2002) A new non-linear normalization method for reducing variability in DNA microarray experiments. *Genome Biol* **3:** research 0048.

Zhang Y, Dawson MI, Mohammad R, Rishi AK, Farhana L, Feng KC, Leid M, Peterson V, Zhang XK, Edelstein M, et al. (2002) Induction of apoptosis in retinoid-refractory acute myelogenous leukemia by a novel AHPN analog. *Blood* **100:**2917–2925.

Zhao X, Demary K, Wong L, Vaziri C, McKenzie AB, Eberlein TJ, and Spanjaard RA (2001) Retinoic acid receptor-independent mechanism of apoptosis of melanoma cells by the retinoid CD437 (AHPN). *Cell Death Differ* **8:**878–886.

Zhuang Y, Faria TN, Chambon P, and Gudas LJ (2003) Identification and characterization of retinoic acid receptor beta2 target genes in F9 teratocarcinoma cells. *Mol Cancer Res* **1:**619–630.

Zuco V, Zanchi C, Cassinelli G, Lanzi C, Supino R, Pisano C, Zanier R, Giordano V, Garattini E, and Zunino F (2004) Induction of apoptosis and stress response in ovarian carcinoma cell lines treated with ST1926, an atypical retinoid. *Cell Death Differ* **11:**280–289.

Address correspondence to: Enrico Garattini, Laboratory of Molecular Biology, Centro Catullo e Daniela Borgomainerio, Istituto di Ricerche Farmacologiche "Mario Negri", via Eritrea 62, 20157 Milano, Italy. E-mail: egarattini@marionegri.it